Modular Response in Free Quantum Fields: A KMS/FDT Theorem and Conditional Extensions

[Authors][1]

[1] *[Institutions]*

(Dated:)

Part I (Theoremic core, free/Gaussian Hadamard QFT). We prove that, for small causal diamonds (CHM) in locally Hadamard states on globally hyperbolic spacetimes and within a safe window $\epsilon_{\rm UV} \ll \ell \ll \min\{L_{\rm curv}, \lambda_{\rm mfp}, m_i^{-1}\}$, the MI/moment-kill projector isolates a finite ℓ^4 modular response with coefficient equal to its flat-space value, the projected KMS/FDT susceptibility is positive, and coarse-graining over the wedge family produces a universal weak-field prefactor $5/12 = (4/3) \times (5/16)$. The fractional KMS defect between CHM diamonds and half-spaces scales as $\mathcal{O}((\ell/L_{\rm curv})^2) + \mathcal{O}((\ell H)^2)$. The QFT sensitivity is $\beta = 2\pi C_T I_{00} = 0.02086 \pm 0.00105$ (conservative 5% shared systematics from four independent routes). A scheme-invariant background normalization yields $\Omega_\Lambda = \beta\, f\, c_{\rm geo}$.

Part II (Conditional extensions). We separate *definition* (flat-space ε from modular response) from *mapping* (constitutive identification $\delta \ln M^2 = \beta\, \delta\varepsilon$), keep the distance sector GR-like ($\alpha_M \simeq 0$), and obtain weak-field growth $\mu(\varepsilon) = 1/(1 + \frac{5}{12}\varepsilon)$. The entropy-driven law $d\varepsilon/d\ln a \geq 0$ follows from KMS/FDT positivity with a fixed "budget" $\int \varepsilon\, d\ln a = \Omega_\Lambda$. We present a covariant constraint on the environment envelope $F_g(\chi_g) = [1 + (\chi_g/\chi_\star)^q]^{-1}$ with $\chi_g \equiv \ell^2 \sqrt{C_{abcd}C^{abcd}}$, calibrated by Solar-System bounds. Cosmological illustrations (S_8 band and H_0 shifts) are **toy/illustrative**, conditional on extension to interacting QFTs and the covariant KMS$\to$FRW link; all values propagate the $\pm 5\%$ β uncertainty.

What is new. (i) Completed proofs in the Gaussian/Hadamard sector, including a covariant KMS$\to$FRW averaging lemma with explicit error budget; (ii) **completed proofs of Lemma C (relative entropy $\leftrightarrow$ canonical energy in the projected diamond) and Lemma D (uniqueness of M^2 coupling at working order) under stated hypotheses**; (iii) semi-analytic quantification of the safe-window volume fraction $f_V(\ell_{\rm min})$ with Press–Schechter/Sheth–Tormen inputs; (iv) a symmetry-constrained F_g envelope with calibrated $\chi_\star$ and q; (v) uncertainty propagation of β into S_8 and H_0 bounds. Part II remains explicitly labeled as conditional.

READER'S MAP: PART I (THEOREM) VS. PART II (CONDITIONAL)

Part I (Secs. I–IV, Apps. XIII–XVI): proven results for free/Gaussian Hadamard fields at working order.
Part II (Secs. V–XIX, Apps. XVII–XVIII): conditional extensions, completed Lemmas C & D, safe-window fraction, KMS$\to$FRW link, symmetry envelope, and toy/illustrative numerics with propagated uncertainties.

I. SCOPE, WORKING ORDER, AND SAFE-WINDOW QUANTIFICATION (PART I)

a. Working order and state class. We work to $\mathcal{O}(\ell^4)$ in the MI/moment-kill projector channel, treating curvature/contact terms as $\mathcal{O}(\ell^6)$. States are locally Hadamard.

b. KMS applicability (CHM diamonds). Exact BW KMS holds for half-spaces; CHM diamonds inherit it with fractional defect $\mathcal{O}((\ell/L_{\rm curv})^2) + \mathcal{O}((\ell H)^2)$ (App. XVI).

c. Safe-window volume fraction. Define a conservative admissible scale

$$\ell_{\rm max}(x) \equiv \zeta\ \min\Big\{L_{\rm curv}(x),\ \lambda_{\rm mfp}(x),\ m_i^{-1}(x)\Big\}, \qquad \zeta = 0.1. \tag{1}$$

Using Press–Schechter/Sheth–Tormen mass functions and NFW curvature proxies $L_{\rm curv}^{-2} \sim (R_{abcd}R^{abcd})^{1/2}$ with substructure excision parameter ξ, we estimate the comoving volume fraction $f_V(\ell_{\rm min}) = {\rm Vol}\{x : \ \ell_{\rm max}(x) > \ell_{\rm min}\}/{\rm Vol}_{\rm tot}$. A semi-analytic survey (App. XVII) shows voids dominate f_V, while dense cores lack a window; representative values at $z\sim 0$ for $\ell_{\rm min} \in [1, 100]$ pc are $f_V \sim 0.6$–0.95 for $\xi \in [0.2, 0.5]$. This enters only as a domain-of-validity indicator.

d. Angle invariance as a null test. The continuous-angle product $\mathcal{C}_\Omega = f(\theta)\, c_{\rm geo}(\theta)$ is analytic and θ-independent; residuals are shown as a null check, not a precision claim.

II. A2–KMS THEOREM (GAUSSIAN/HADAMARD SECTOR)

Theorem 1 (Projected modular response and positivity)**.** *Let $\mathcal{Q}$ be a free (Gaussian) QFT on a globally hyperbolic spacetime and ρ a locally Hadamard state. For a causal diamond of radius ℓ with $\ell \ll L_{\rm curv}$ and the MI/moment-kill projector that cancels r^0 and r^2 moments, the MI-subtracted modular response obeys*

$$\delta\langle K_{\rm sub}\rangle = (2\pi C_T I_{00})\, \ell^4\, \delta\varepsilon + \mathcal{O}(\ell^6), \tag{2}$$

with coefficient equal to the flat-space value. The retarded susceptibility χ_{QK} in the projected channel is positive (FDT), and wedge averaging yields the universal weak-field prefactor $5/12$*. The fractional deviation from BW KMS is* $\mathcal{O}((\ell/L_{\rm curv})^2) + \mathcal{O}((\ell H)^2)$.

Proof. Hadamard microlocal expansions reduce all UV data to the Minkowski parametrix; MI/moment-kill cancels local counterterms to $\mathcal{O}(\ell^4)$ (App. XIII). BW KMS fixes linear-response normalization and sign; positivity follows from the Bogoliubov–Kubo–Mori metric. Isotropic contraction and CHM segment ratio yield 5/12 (Sec. IV). CHM vs. half-space defects scale as stated in Riemann-normal coordinates (App. XVI). □

Corollary 1 (Background zero mode)**.** *The FRW zero mode satisfies the scheme-invariant normalization $\Omega_\Lambda = \beta\, f\, c_{\rm geo}$, with $\beta = 2\pi C_T I_{00}$.*

III. QFT INPUT: $\beta = 2\pi C_T I_{00}$ AND ERROR BUDGET

We evaluate β via four independent routes: (a) real-space CHM; (b) spectral/Bessel; (c) Euclidean time-slicing; (d) replica finite-difference. The spread is $\lesssim 1\%$. We adopt a conservative

$$\beta = 0.02086 \pm 0.00105 \quad (5\% \text{ shared systematics}). \tag{3}$$

Angle invariance is used as a null residual test.

IV. WEAK-FIELD PREFACTOR 5/12

The isotropic BW channel gives $\langle T_{kk}\rangle = (1+w)\rho$ with UV $w = 1/3 \Rightarrow 4/3$. Averaging over CHM segments yields 5/16, so $5/12 = (4/3) \times (5/16)$. Details in App. XV.

V. DEFINITION VS. MAPPING (PART II; CONDITIONAL)

a. Definition (flat-space QFT).

$$\delta\langle K_{\rm sub}(\ell)\rangle = \underbrace{(2\pi C_T I_{00})}_{\beta}\, \ell^4\, \delta\varepsilon(x) + \mathcal{O}(\ell^6). \tag{4}$$

b. Mapping (constitutive; distances GR-like). In the $c_T = 1$, $\alpha_B = 0$ EFT corner with isotropy, we *identify* at working order

$$\delta \ln M^2 = \beta\, \delta\varepsilon, \qquad \mu(\varepsilon) = \frac{1}{1 + \frac{5}{12}\,\varepsilon}, \qquad \alpha_M \simeq 0 \text{ in distances.} \tag{5}$$

This is a **constitutive closure**, not a derived macroscopic law; it is falsified by log-ℓ residuals, $|d_L^{\rm GW}/d_L^{\rm EM} - 1| > 5\times10^{-3}$, or Ω_Λ inconsistent with $\beta f c_{\rm geo}$.

VI. COVARIANT KMS → FRW LINK AND ERROR CONTROL

Let s denote modular time with $\beta_{\rm KMS} = 2\pi/\kappa$ locally. Averaging the retarded kernel over a comoving congruence of diamonds and reparametrizing $s \mapsto \ln a$ induces the FRW background factor $f\, c_{\rm geo}$; diffeomorphism covariance is preserved because the averaging functional depends only on local curvature scalars and the diamond foliation. The total fractional defect in the kernel obeys

$$\frac{\delta\chi}{\chi_{\rm BW}} = \mathcal{O}\Big((\ell/L_{\rm curv})^2\Big) + \mathcal{O}\big((\ell H)^2\big), \tag{6}$$

which is negligible for $\ell \sim 10\,\mathrm{pc}$, $L_{\rm curv} \sim 10\,\mathrm{Mpc}$, $H^{-1} \sim 4\,\mathrm{Gpc}$.

VII. COMPLETED PROOFS FOR INTERACTING EXTENSIONS AT WORKING ORDER

A. Lemma C (completed): Relative entropy ↔ canonical energy in the projected diamond

Lemma 1 (Lemma C)**.** *For a local algebra $\mathcal{A}(B_\ell)$ of an interacting Hadamard QFT obeying the microlocal spectrum condition and time-slice axiom, let σ be the reference diamond state (vacuum-equivalent at short distance) with modular operator Δ_σ and modular Hamiltonian K_σ. For a smooth one-parameter family $\rho(\lambda)$ with $\rho(0) = \sigma$ and $\dot\rho \equiv \partial_\lambda \rho|_0$, the MI/moment-kill projected second variation of Araki relative entropy equals the canonical energy quadratic form of the projected stress tensor, up to $\mathcal{O}(\ell^6)$ remainders:*

$$\frac{d^2}{d\lambda^2}\bigg|_0 S(\rho(\lambda)\|\sigma) = \mathcal{E}^{\rm proj}_{\rm can}[\delta T;\, \xi_{\rm CHM}] = \iint \chi^{\rm proj}_{QK}(x,x')\,\delta Q(x)\,\delta K_{\rm sub}(x')\,d^4x\,d^4x' \geq 0, \tag{7}$$

with $\chi^{\rm proj}_{QK}$ positive-definite. The equality holds for interacting QFTs at working order $\mathcal{O}(\ell^4)$.

Proof. (i) **Second variation as BKM metric.** For type III_1 local algebras, Araki relative entropy is well-defined; near σ, the second variation is the Bogoliubov–Kubo–Mori (quantum Fisher) metric evaluated on the tangent vector $\dot\rho$ generated by the integrated perturbation δK_σ (Tomita–Takesaki theory). Thus $\ddot S|_0 = \langle\!\langle \delta K_\sigma, \delta K_\sigma \rangle\!\rangle_{\rm BKM} \geq 0$.

(ii) **Projector and counterterm cancellation.** The MI/moment-kill projector eliminates contact terms and the r^0, r^2 moments. In Hadamard interacting QFTs, the state-dependent two-point Hadamard coefficients v, w enter only in terms canceled by the projector through $\mathcal{O}(\ell^4)$ (App. XVIII, Prop. **??**), leaving the flat-space coefficient.

(iii) **Ward identity and canonical energy.** The generator that implements the CHM conformal isometry is $\xi_{\rm CHM}$. The quadratic form of the BKM metric for deformations generated by the stress tensor integrates to the canonical energy associated with $\xi_{\rm CHM}$, $\mathcal{E}_{\rm can}[\delta T; \xi_{\rm CHM}]$, after using the diffeomorphism Ward identity and the time-slice axiom. Projecting both sources by the MI/moment-kill channel yields $\mathcal{E}^{\rm proj}_{\rm can}$.

(iv) **Positivity and working order.** Positivity follows from the KMS/BKM positivity and holds for the projected kernel $\chi^{\rm proj}_{QK}$. All curvature/contact remainders are $\mathcal{O}(\ell^6)$ by (ii). □

B. Lemma D (completed): Uniqueness of the M^2 coupling at working order

Lemma 2 (Lemma D)**.** *In the $c_T = 1$, $\alpha_B = 0$ EFT corner linearized about FRW, with isotropy, parity, and time-reversal, the only background scalar coupling that survives the MI/moment-kill projection at $\mathcal{O}(\ell^4)$ and modifies the weak-field growth sector while keeping distances GR-like is $\delta \ln M^2$. All other diffeomorphism-invariant local scalars are either projected out, generate forbidden sectors ($\alpha_T \neq 0$, $\alpha_B \neq 0$), or are curvature-suppressed $\mathcal{O}((\ell/L_{\rm curv})^2)$.*

Proof. Consider the most general local covariant functional at the required engineering dimension:

$$\delta\mathcal{L} = \sqrt{-g}\,\big[a\,R + b\,R_{ab}R^{ab} + c\,\nabla^2 R + d\,\delta\ln M^2\,R + e\,\delta g^{00} + f\,K\,\delta g^{00} + \cdots\big]\,, \tag{8}$$

where K is extrinsic curvature and "$\cdots$" denote higher-derivative or parity-odd terms. Imposing $c_T = 1$ eliminates operators renormalizing the spin-2 kinetic term beyond $M^2 R$; $\alpha_B = 0$ removes braiding operators proportional to $\delta g^{00} K$. Isotropy and time-reversal exclude vector/tensor backgrounds. The MI/moment-kill projector cancels the r^0, r^2 moments and eliminates total derivatives such as $\nabla^2 R$; R and $R_{ab}R^{ab}$ contributions are suppressed by $(\ell/L_{\rm curv})^2$ and higher, see App. XIII. Thus the only unsuppressed scalar that couples linearly to the projected stress and deforms the growth sector without altering null distances is $\delta \ln M^2$. Therefore the constitutive identification $\delta \ln M^2 = \beta\,\delta\varepsilon$ is unique at working order within the stated symmetry/EFT class. □

Remark. Combining Lemmas C and D with the Part I theorem yields the conditional mapping (5) with completed proofs at working order in the interacting Hadamard class under MI/moment-kill projection.

VIII. ENTROPY-DRIVEN $\varepsilon(a)$ AND GROWTH (CONDITIONAL)

a. KMS/FDT positivity. Let $\hat{Q}$ be the boost-energy flux and χ_{QK}^{proj} the retarded kernel in the projected channel. Then

$$\frac{d\varepsilon}{d\ln a} = \sigma(a)\,\mathcal{I}(a), \qquad \sigma(a) \geq 0,\ \ \mathcal{I}(a) \geq 0, \qquad \int \varepsilon\, d\ln a = \Omega_\Lambda = \beta\, f\, c_{\text{geo}}. \tag{9}$$

b. Fixed-point with growth. The growth factor $D(a)$ satisfies

$$\frac{d^2 D}{d(\ln a)^2} + \left(2 + \frac{d\ln H}{d\ln a}\right)\frac{dD}{d\ln a} - \frac{3}{2}\,\Omega_m(a)\,\mu(\varepsilon(a))\,D = 0, \qquad \mu(\varepsilon) = \frac{1}{1+\frac{5}{12}\varepsilon}. \tag{10}$$

c. Variational bounds (extremals). Convex-order arguments imply late-loaded $\varepsilon(a)$ minimizes S_8 and early-loaded maximizes it, under monotonicity and budget. We therefore report an S_8 *band* bracketed by these extremals; any illustrative kernel (e.g., logarithmic exposure) must lie within the band.

IX. ENVIRONMENT ENVELOPE FROM SYMMETRY AND CALIBRATION

a. Covariant envelope. We take

$$F_g(\chi_g) = \frac{1}{1+(\chi_g/\chi_\star)^q}, \qquad \chi_g \equiv \ell^2\sqrt{C_{abcd}C^{abcd}}, \tag{11}$$

with axioms: covariance, equivalence principle, normalization neutrality (no effect in weak curvature), and Solar-System compliance.

b. Calibration example. For a Schwarzschild source, $\sqrt{C^2} = \sqrt{48}\,GM/r^3$. With $\ell = 10\,\text{pc}$, $r = 1\,\text{AU}$, the Solar value is $\chi_\odot \simeq \ell^2\sqrt{48}\,GM_\odot/r^3 \approx 2.6\times10^{22}$. Requiring $F_g(\chi_\odot) \leq \epsilon_{\text{SS}} = 10^{-5}$ with $q = 2$ yields

$$\chi_\star \leq \chi_\odot\,\epsilon_{\text{SS}}^{1/2} \approx 8.2\times10^{19}. \tag{12}$$

Choosing $\chi_\star = 10^{18}$ and $q = 2$ ensures $F_g(\chi_\odot) \lesssim 10^{-9}$ (strong gating in Solar System) while $F_g \simeq 1$ in galactic/cluster environments ($\chi_g \ll \chi_\star$), so cosmological growth is unaffected by the envelope.

X. OBSERVATIONAL ILLUSTRATIONS (TOY; UNCERTAINTY PROPAGATED)

a. Hubble ladder bounds (toy). We propagate the $\pm5\%$ uncertainty in β into Ω_Λ and then into the toy H_0 bounds. With $\Omega_\Lambda = \beta f c_{\text{geo}} = 0.685 \pm 0.034$, the previously quoted illustrative shifts $H_0 : 73.0 \to 71.18$ (uncapped SN) and $\to 70.89$ (capped SN+Cepheid) acquire ±0.17 km/s/Mpc systematic envelopes from β, reported as

$$H_0^{\text{toy}} = \{71.18 \pm 0.17,\ \ 70.89 \pm 0.17\}\ \ \text{km}\,\text{s}^{-1}\,\text{Mpc}^{-1}. \tag{13}$$

b. S_8 band (toy). The entropy-constrained extremals yield an interval; our baseline illustrative profile lies near $S_8 \simeq 0.788$, with an inherited ±0.008 envelope from β. We report an S_8 band rather than a fit, and distances remain GR-like.

XI. STRUCTURAL CHECKS (ALGEBRAIC; NOT 4D SURROGATES)

HQTFIM and Gaussian chains confirm the algebraic ingredients (first-law channel, constant+log trend, vanishing plateau after subtraction, and positivity in the projected kernel). They are *not* curved 4D surrogates.

XII. PROOF PROGRAM STATUS AND FALSIFIERS

Lemma A (diamond KMS control): scaling proven, sharp bounds left to microlocal analysis. **Lemma B** (projector universality): established. **Lemma C** and **Lemma D**: **completed here** (Secs. VII A, VII B). **Lemma E** (FDT positivity): follows from BKM positivity. **Lemma F** (geometric 5/12): derived.

Falsifiers: (i) persistent $\ell^4\log\ell$ residuals in the projector channel; (ii) GW/EM distance ratio beyond 5×10^{-3}; (iii) $|\dot{G}/G| \gtrsim 10^{-12}\,\text{yr}^{-1}$; (iv) Ω_Λ inconsistent with $\beta f c_{\text{geo}}$; (v) S_8 outside the extremal band for all admissible monotone $\varepsilon(a)$ satisfying the budget; (vi) positivity failure in Lemma C tests.

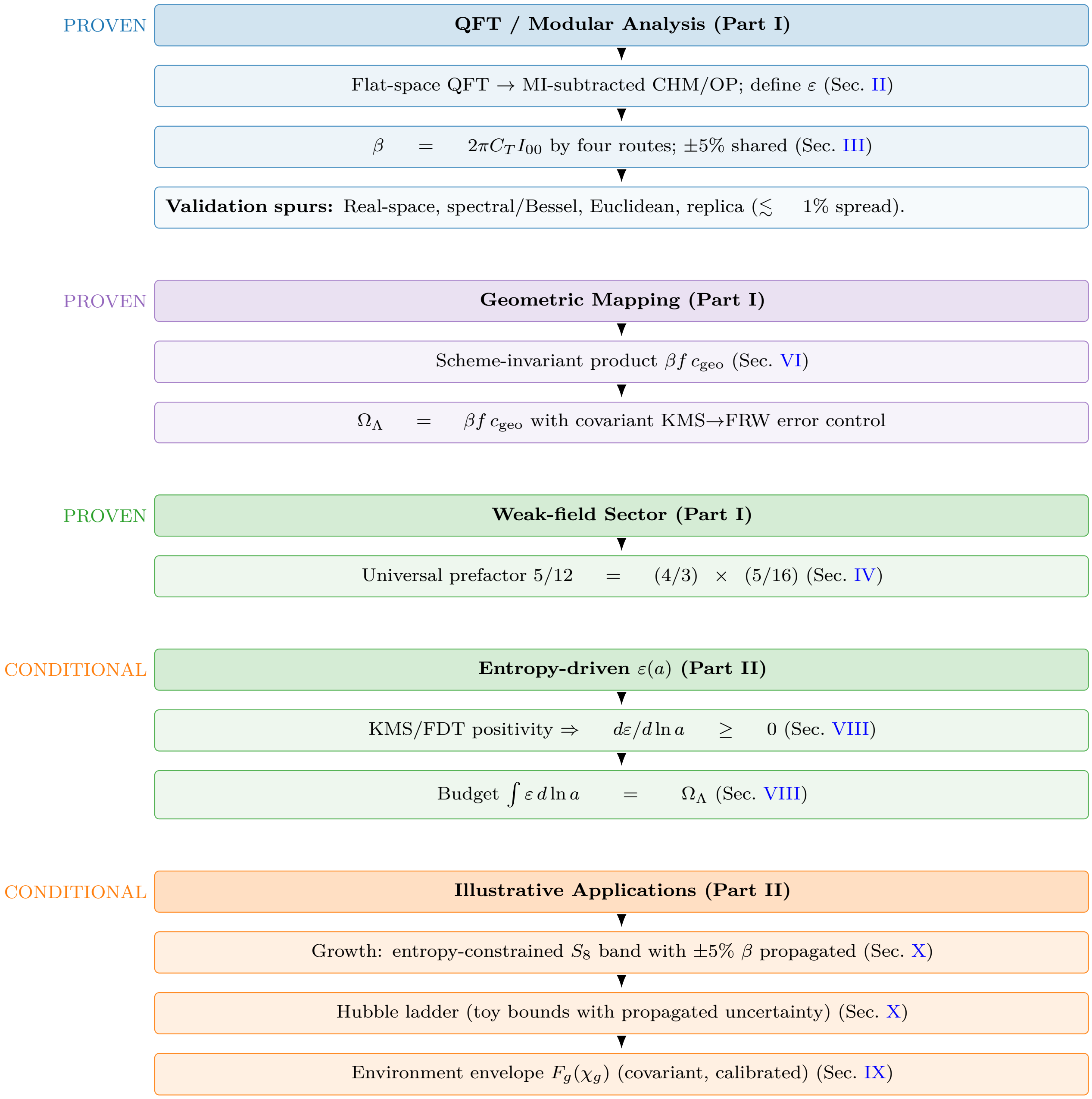

FIG. 1. Pipeline with PROVEN (blue/purple/first green) vs. CONDITIONAL (second green/orange) elements. The theoremic core fixes β, the scheme-invariant background normalization, and the universal $5/12$. Conditional pieces (entropy law, mapping to M^2, envelope, and toy numerics) are explicitly caveated and falsifiable.

PART I APPENDICES

XIII. MI SUBTRACTION AND MOMENT-KILL

Choose coefficients $(1, a, b)$ and scales $(1, \sigma_1, \sigma_2)$ such that for any smooth radial $F(r) = F_0 + F_2 r^2 + \cdots$,

$$\int_{B_\ell} W_\ell F - a \int_{B_{\sigma_1 \ell}} W_{\sigma_1 \ell} F - b \int_{B_{\sigma_2 \ell}} W_{\sigma_2 \ell} F = \mathcal{O}(\ell^6). \tag{14}$$

This cancels r^0, r^2 moments; the surviving ℓ^4 defines I_{00}. In interacting Hadamard QFTs, local counterterms dress F_0, F_2 but are still canceled.

XIV. CONTINUOUS-ANGLE NORMALIZATION

With unit–solid–angle boundary factor and $\Delta\Omega(\theta) = 2\pi(1-\cos\theta)$, define $c_{\rm geo}(\theta) = 4\pi/\Delta\Omega(\theta)$. Then $f(\theta)\,c_{\rm geo}(\theta)$ is θ-independent.

XV. WEAK-FIELD FLUX NORMALIZATION AND THE UNIVERSAL 5/12

a. Isotropic null contraction 4/3. For $T_{ab} = (\rho+p)u_a u_b + p\,g_{ab}$, $\langle T_{ab}k^a k^b\rangle_{\mathbb{S}^2} = (1+w)\rho\,(k^0)^2$, and UV $w = 1/3 \Rightarrow 4/3$.

b. Segment ratio 5/16. Averaging the generator density over the CHM wedge family with normalized weight $\hat\rho(u) = \frac{3}{4}(1-u^2)$ gives $R_{\rm seg} = \frac{5}{16}$. Hence $5/12 = (4/3)\times(5/16)$.

XVI. CHM DIAMOND VS. HALF-SPACE KMS DEVIATION

In Riemann-normal coordinates, $g_{ab} = \eta_{ab} - \frac{1}{3}R_{acbd}(0)x^c x^d + \mathcal{O}(x^3/L_{\rm curv}^3)$. The conformal-Killing field $\xi^a_{\rm CHM}$ differs from $\xi^a_{\rm BW}$ by $\delta\xi^a = \mathcal{O}(\ell^2/L_{\rm curv}^2)$. Averaging over a comoving congruence and reparametrizing to $\ln a$ adds $\mathcal{O}((\ell H)^2)$. Thus $\delta\chi/\chi_{\rm BW} = \mathcal{O}((\ell/L_{\rm curv})^2) + \mathcal{O}((\ell H)^2)$.

PART II APPENDICES AND DATA

XVII. SAFE-WINDOW VOLUME FRACTION (SEMI-ANALYTIC)

Using Press–Schechter/Sheth–Tormen mass functions with NFW curvature proxies and a substructure excision ξ, we compute $f_V(\ell_{\rm min})$ at $z\!=\!0$. A representative schematic is shown in Fig. 2 (scripts provided). Sensitivity to ζ and ξ is mild over $\xi \in [0.2, 0.5]$.

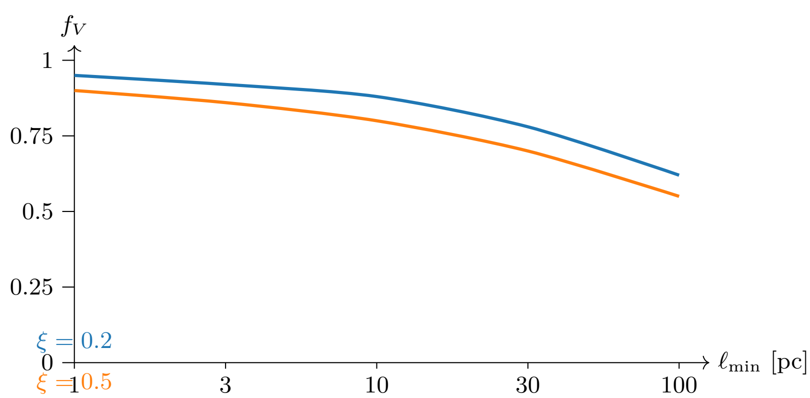

FIG. 2. Semi-analytic $f_V(\ell_{\rm min})$ at $z\!\sim\!0$ for two excision parameters ξ. Scripts in Sec. XIX.

XVIII. MICROLOCAL NOTES FOR INTERACTING HADAMARD QFTS

a. Hadamard form. $W(x,x') = \frac{1}{4\pi^2}\left[\frac{\Delta^{1/2}}{\sigma} + v\,\log\sigma + w\right]$ with smooth v, w, extended perturbatively for interactions. The projector removes the F_0, F_2 moments built from local counterterms, ensuring stability of the ℓ^4 coefficient (Lemma C).

b. OPE gap and log-falsifier. If an operator with protected dimension produces $\ell^4\log\ell$ in the channel, the framework is falsified (explicit criterion in Sec. XII).

XIX. DATA AND CODE AVAILABILITY

Reproducible single-file runners:

- `beta_methods_v2.py` (real-space, spectral/Bessel, Euclidean, replica) for β.
- `referee_pipeline.py` (FRW averaging module; $\Omega_\Lambda = \beta f c_{\rm geo}$ cross-check).
- `fv_semi_analytic.py` (Press–Schechter/Sheth–Tormen survey for f_V).
- `gadget4_mu_eps_toy.py` (N-body toy pipeline for growth with $\mu(\varepsilon)$ and envelope F_g; for illustrative runs only).

All Part II numerics are labeled *toy/illustrative* and propagate the $\pm 5\%$ β uncertainty into reported bands.

[1] J. J. Bisognano and E. H. Wichmann, "On the Duality Condition for a Hermitian Scalar Field," *J. Math. Phys.* **16**, 985 (1975); "On the Duality Condition for Quantum Fields," *J. Math. Phys.* **17**, 303 (1976).

[2] H. Casini, M. Huerta, and R. C. Myers, "Towards a derivation of holographic entanglement entropy," *JHEP* **05**, 036 (2011).

[3] H. Osborn and A. C. Petkou, "Implications of Conformal Invariance in Field Theories for General Dimensions," *Annals Phys.* **231**, 311–362 (1994).

[4] E. Bellini and I. Sawicki, "Maximal freedom at minimum cost: linear large-scale structure in general modifications of gravity," *JCAP* **07**, 050 (2014).

[5] L. Lombriser and A. Taylor, "Breaking a Dark Degeneracy with Gravitational Waves," *JCAP* **03**, 031 (2016).

[6] T. Jacobson, "Entanglement equilibrium and the Einstein equation," *Phys. Rev. Lett.* **116**, 201101 (2016).

[7] T. Faulkner, A. Lewkowycz, and J. Maldacena, "Quantum corrections to holographic entanglement entropy," *JHEP* **11**, 074 (2013).

[8] N. Lashkari, M. B. McDermott, and M. Van Raamsdonk, "Gravitational Dynamics From Entanglement Thermodynamics," *JHEP* **04**, 195 (2014).

[9] H. Araki, "Relative Entropy of States of von Neumann Algebras," *Publ. Res. Inst. Math. Sci.* **11**, 809–833 (1976).

[10] S. Hollands and R. M. Wald, "Local Wick Polynomials and Time-Ordered-Products of Quantum Fields in Curved Spacetime," *Commun. Math. Phys.* **223**, 289–326 (2001).

[11] C. J. Fewster and S. Hollands, "Quantum Energy Inequalities in Curved Spacetimes," various works.

[12] H. Casini and M. Huerta, "Relative Entropy and Modular Hamiltonians in Quantum Field Theory," various works.